

## The generation of reactive-oxygen species associated with long-lasting pulse-induced electroporabilisation of mammalian cells is based on a non-destructive alteration of the plasma membrane

Pierre Bonnafe, Marie-Christine Vernhes, Justin Teissie, Bruno Gabriel \*

*Institut de Pharmacologie et de Biologie Structurale du CNRS, UPR 9062, Toulouse, France*

Received 21 June 1999; received in revised form 25 August 1999; accepted 7 September 1999

### Abstract

Chinese hamster ovary (CHO) cells in suspension were subjected to pulsed electric fields suitable for electrically mediated gene transfer (pulse duration longer than 1 ms). Using the chemiluminescence probe lucigenin, we showed that a generation of reactive-oxygen species (oxidative jump) was present when the cells were electroporabilised using millisecond pulses. The oxidative jump yield was controlled by the extent of alterations allowing permeabilisation within the electrically affected cell area, but showed a saturating dependence on the pulse duration over 1 ms. Cell electroporation induced reversible and irreversible alterations of the membrane assembly. The oxidative stress was only present when the membrane permeabilisation was reversible. Irreversible electrical membrane disruption inhibited the oxidative jump. The oxidative jump was not a simple feedback effect of membrane electroporabilisation. It strongly controlled long-term cell survival. This had to be associated with the cell-damaging action of reactive-oxygen species. However, for millisecond-cumulated pulse duration, an accumulation of a large number of short pulses (microsecond) was extremely lethal for cells, while no correlation with an increased oxidative jump was found. Cell responses, such as the production of free radicals, were present during electroporabilisation of living cells and controlled partially the long-term behaviour of the pulsed cell. © 1999 Elsevier Science B.V. All rights reserved.

**Keywords:** Electroporabilisation; Electroporation; Membrane electric potential difference; Oxidative injury; Reactive oxygen species; Cell death

Abbreviations: CHO, Chinese hamster ovary; CL, lucigenin-dependent chemiluminescence;  $E$ , electric field intensity;  $E_p(T)$ , apparent electric field threshold triggering electroporabilisation;  $E_{ch}(T)$ , apparent electric field threshold triggering chemiluminescence;  $E_s$ , critical electric field threshold triggering electroporabilisation on the cell side facing the anode;  $E_F$ , critical electric field threshold triggering electroporabilisation on the cell side facing the cathode;  $T$ , duration of pulse;  $D$ , delay between pulses; DMF, dimethylformamide; ROS, reactive-oxygen species; (Pam)Afluorescein, 5-(*N*-hexadecanoyl)-aminofluorescein;  $k_{ox}$ , apparent oxidation rate constant of (Pam)Afluorescein;  $k_p$ ,  $k_{ox}$  measured on living electroporabilised cells;  $k_d$ ,  $k_{ox}$  measured on irreversibly electroporabilised cells;  $k_o$ ,  $k_{ox}$  measured on control cells;  $k_1$ , oxidation rate constant of (Pam)Afluorescein inserted in native plasma membrane;  $k_2$ , oxidation rate constant of (Pam)Afluorescein inserted in electroporabilised plasma membrane parts;  $I_f$ , intensity of the fluorescence signal;  $I_{fp}$ ,  $I_f$  measured on living electroporabilised cells;  $I_{fd}$ ,  $I_f$  measured on irreversibly electroporabilised cells;  $I_{fo}$ ,  $I_f$  measured on control cells

\* Corresponding author. IPBS-CNRS, 205 route de Narbonne, F-31077 Toulouse cedex 4, France. Fax: +33-5-6133-5860; E-mail: gabriel@ipbs.fr

## 1. Introduction

Methods for reversible permeabilisation of the cell membrane have been actively developed, based on various techniques for exogenous molecule delivery into the living cell [1]. Electrically induced membrane permeabilisation is a simple ubiquitous method which yields a high amount of delivered molecules [2]. Application of brief (micro- to millisecond) intense (hundreds of V/cm) external electric field pulses to living cells (electropulsation) can make the plasma membrane transiently permeable (electropermeabilisation or electroporation). Electropermeabilisation is now frequently used in biology and medicine to introduce *in vivo* exogenous active small compounds, such as drugs (electrochemotherapy) [3], or macromolecules, such as proteins or nucleic acids (electromediated gene delivery) [4], and to transport molecules across tissues for therapeutic purpose (e.g. transdermal delivery) [5]. Therefore, a clear understanding of the physical and structural bases of electropermeabilisation, and cell responses associated with this transient state of the plasma membrane is a necessity.

The driving force involved in electropermeabilisation is a localised increase in the trans-membrane electric potential difference which, when larger than a threshold value (between 0.25 and 0.5 V) [6,7] triggers a change in the permeability properties of the membrane [8]. On the cell surface membrane, electropermeabilisation remains local and the part of the cell membrane area affected by the electrical treatment depends on the applied field strength [9,10]. But the intrinsic level of permeabilisation in this local region depends on the pulse duration and number [7,11,12].

Permeabilisation of the cell plasma membrane can modulate the native functional properties of the cell. In the case of immune cells, it was shown that exposure to an external electric field intensifies the oxidative burst in lymphocytes [13], macrophages [14], and neutrophils [15,16]. It was suggested that such oxidative burst exaltations were the result of electro-induced influx of external calcium ions into the permeabilised cell [17].

In a previous study with Chinese hamster ovary (CHO) cells, we demonstrated the existence of a generation of reactive-oxygen species (ROS) induced by

short-pulse induced membrane electropermeabilisation (oxidative jump) [18]. Such an oxidative jump attributed to Haber–Weiss reaction-mediated hydroxyl radical formation in the electropermeabilised cell was afterwards generalised to various non-phagocytic cell types, such as plant protoplast [19], intact plant cell [20], and yeast [21]. A strong correlation was revealed between cell survival after the electric treatment and oxidative jump intensity, in the case of CHO cells. Using single cell analysis, we gave direct evidence of membrane localisation of electrogenerated ROS [22]. An increase of lipid peroxidation in membranes after electropermeabilisation has been reported [23]. The electropermeabilisation process must not be simply described as aqueous pathways through the lipid matrix of the plasma membrane, but cell responses associated with this transient state of the membrane must be considered. Systematic characterisation and analysis of these cellular contributions was a necessity to understanding the basis of electropermeabilisation.

Short-duration pulses are ineffective for electro-mediated DNA transfer except if high electric field intensities are used [24]. The pulse duration is a crucial parameter in the electro-mediated process. The mechanisms of membrane permeabilisation using short pulse and long pulse were reported as fundamentally different [12,25]. It clearly appears nowadays that better *in vitro* electro-mediated DNA transfer into living cells is achieved with long-pulse durations ( $> 1$  ms) [12,26–29]. However, side effects of electropermeabilisation, such as damage in cell DNA [30] and oxidative stress [18], need to be taken into account to optimise the electrical parameters for efficient electro-mediated DNA transfer. In the present study, using lucigenin-dependent chemiluminescence (CL) measurements and an original photo-oxidation assay, we characterise the oxidative jump present when CHO cells are electropermeabilised using long-lasting pulses, i.e. using (1) ms pulses and (2) trains of  $\mu$ s pulses with ms-cumulated duration.

## 2. Materials and methods

### 2.1. Materials

10,10'-Dimethyl-9,9'-bisacridinium dinitrate (luci-

genin) and Direct-blue (D-2535) were obtained from Sigma (St Louis, MO). (5-(*N*-Hexadecanoyl)-amino-fluorescein ((Pam)Afluorescein) was purchased from Molecular Probes (Eugene, OR). Crystal violet (CI 42555) was obtained from Merck (Darmstadt, Germany). Salts and solvents were of analytical grade. Buffer A (pulsing buffer) was 250 mM sucrose, 10 mM  $\text{KH}_2\text{PO}_4/\text{K}_2\text{HPO}_4$ , pH 7.4, and 1 mM  $\text{MgCl}_2$ . Buffer B was 138 mM NaCl, 3 mM KCl, 1.5 mM  $\text{KH}_2\text{PO}_4$ , 8 mM  $\text{Na}_2\text{HPO}_4$ , pH 7.4. The free calcium ion concentration in the two buffers was 3–5  $\mu\text{M}$ .

## 2.2. Cell culture

CHO cells (WTT clone) were grown in suspension in completed Eagle's minimum essential medium (MEM 0111, Eurobio, Les Ulis, France) to avoid trypsin treatment, as previously described [18]. They were maintained in exponential growth (4–10  $10^5$  cells/ml) by daily dilution in the culture medium. Cells grown in suspension can be replated readily on Petri dishes and kept at 37°C in a 5%  $\text{CO}_2$  incubator (Jouan, St Herblain, France) to grow as monolayers.

During this study (see Fig. 8), a lower cell sensitivity to the electric field was observed with cell culture ageing (i.e. the number of cell passages). This was probably the result of changes in the physical parameters of the plasma membrane as previously reported [31,32]. Experimental parameters were then accordingly adjusted.

## 2.3. Cell electroporability

The method of cell electroporability was as previously described [18]. Cells in suspension were harvested by centrifugation for 5–10 min at  $100\times g$ , washed twice, and resuspended in buffer A. Electroporability was performed using a CNRS electropulser (Jouan) which delivered DC square-wave pulses with independently adjustable electric parameters (voltage, number of pulses, duration of pulse, and frequency). Pulse parameters were monitored through a 15-MHz oscilloscope (Enertec, St Etienne, France). Cell electroporability was performed at 21°C. A 100- $\mu\text{l}$  amount of cell suspension ( $10^6$  cells) was placed between two stainless-steel parallel electrodes (length 2 cm) seated on the bottom of a

dish. Inter-electrode width was 0.5 cm. The voltage pulse was then applied.

## 2.4. Cell labelling with (Pam)Afluorescein

A 5-mM stock solution of (Pam)Afluorescein was prepared in dimethylformamide (DMF), sheltered from light and stored at 0°C. The cell suspension was harvested by centrifugation, washed twice with buffer B, and the cell pellet was resuspended ( $3\times 10^6$  cells/ml) in the staining solution (10  $\mu\text{M}$  (Pam)Afluorescein in buffer B, with a final DMF concentration of 0.2% (v/v)) for 30 min, at 21°C, and under gentle agitation. After incubation, the cells were centrifuged and the pellet washed twice with buffer A and resuspended in buffer A ( $10^7$  cells/ml).

## 2.5. Determination of electroporability level, and reversibility of electroporability

Electroporability of the cell suspension was quantified by penetration of the impermeant dye Direct-blue (10 mg/ml in buffer A) [30]. Cells were pulsed in Direct-blue (10 mg/ml)-containing buffer A, and observed under an inverted light microscope (Leitz, Wetlar, Germany) after 5 min incubation at room temperature. The percentage of electroporability was determined by counting the number of blue-stained cells compared to the total number of pulsed cells. Reversibility of electroporability was assayed by measuring whether cells could be stained after having been electroporability in buffer A without the dye. Twenty minutes after pulse application, Direct-blue containing buffer A was added to the cell suspension to obtain a final concentration in dye of 10 mg/ml. The suspension was incubated 5 min at room temperature before the percentage of blue-stained cells was counted.

## 2.6. Determination of electropulsed cell viability

Cells ( $2\times 10^5$  cells in 100  $\mu\text{l}$  of sterile buffer A) were pulsed on the bottom of a Petri dish, and kept for 5 min at room temperature. Culture medium (2 ml) was then added. Viability was measured by quantifying the ability of cells to grow as monolayers, over 24 h after electropulsation (more than one generation) by Crystal violet staining [33].

### 2.7. Determination of ROS generated by electropulsed CHO cells

ROS were quantified by lucigenin-chemiluminescence assays using two approaches.

(a) When repetitive short pulses were used, CL was quantified on line with a very sensitive home-built luminometer as previously described [18]. Briefly, 60  $\mu$ l of cell suspension ( $2\text{--}4 \times 10^8$ ) was placed in a special electropulsation chamber and mixed with 10  $\mu$ l of an aqueous 5 mM lucigenin solution. The chamber was then installed in the midst of the luminometer set to maximum gain sensitivity. CL recording was performed in the dark. The CL signal was quantified by time integration (see Appendix A) and reported relative to the maximum signal.

(b) When ms pulses were used, CL was quantified off-line with a luminometer (1250 luminometer, LKB, Turku, Finland) [18]. A 100  $\mu$ l amount of the cell suspension ( $2\text{--}4 \times 10^7$  cells) were pulsed. After pulsation, 30  $\mu$ l of the electroporabilised cell suspension was rapidly mixed with 310  $\mu$ l of buffer A and 10  $\mu$ l of aqueous 5 mM lucigenin solution. The CL recording was started 15 s after electropulsation. The CL signal was characterised by its maximum value ( $I_{\max}$ ).  $I_{\max}$  values were reported as percentages of the maximum value obtained using one 5-ms pulse of 0.9 kV/cm.

### 2.8. Photo-oxidation kinetics of plasma membrane inserted (Pam) Afluorescein

Photo-oxidation kinetics of the dye was observed by fluorescence emission measurement under continuous excitation, at room temperature. The photo-oxidation reaction was monitored by bleaching cells in suspension, as previously described [22]. The pulsation chamber, containing 60  $\mu$ l labelled cell suspension ( $6 \times 10^5$  cells), was placed under a very sensitive fluorimeter build in the laboratory. We used a large bandwidth filter for excitation (390–490 nm, H3 filter block, Leitz), and a narrow bandwidth filter for emission (519 nm,  $\Delta\lambda = 8$  nm; MTO 10313 filter, Massy-Palaiseau, France). Immediately after electropulsation, the fluorescence decay was recorded, cells being uniformly illuminated. The apparent photo-oxidation rate of the cell population was determined by graph analysis.

### 2.9. Statistical analysis of data

DigiMatic 2.05 software (FEB software, Richmond, VA) was run on a Macintosh LC III computer to convert fluorescence decay graphs into digital file. Elsevier-Biosoft computer software 'Linefit' and 'Expofit' were run on an Apple IIe computer to calculate data fittings with linear and exponential behaviour, respectively. Data was the mean  $\pm$  S.D. from at least three independent experiments.

## 3. Results

Electropulsation of CHO cell suspension using single ms pulse induced the generation of ROS (oxidative jump) as previously observed for short pulses ( $\mu$ s) [18].

### 3.1. Electroporabilisation of CHO cells and generation of reactive-oxygen species

Fig. 1 shows the electroporabilisation plot obtained for a CHO cell suspension. Electrical conditions were one pulse of variable duration (0.5–10 ms) and electric field intensity. Electro-induced Direct-blue incorporation into cells was only detected for electric strengths higher than an apparent threshold intensity ( $E_p(T)$ ). This threshold value depended on the pulse duration. Above this apparent threshold

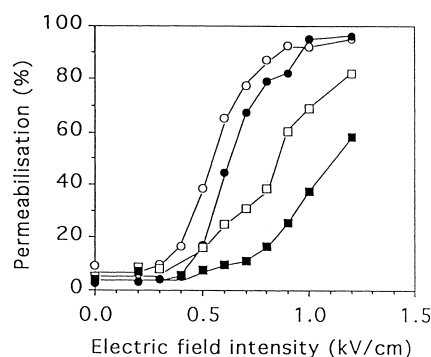


Fig. 1. Effect of long-pulse electric field intensity on the extent of cell permeabilisation. Cell suspensions ( $10^7$  cells/ml) received one single electric pulse of 0.5 ms (■), 1 ms (□), 5 ms (●), and 10 ms (○) in buffer A with 1% Direct-blue. Electroporabilisation was monitored 5 min after pulsation by Direct-blue assay. Average standard deviations on each point were about 10% and were not presented to prevent figure overloading.

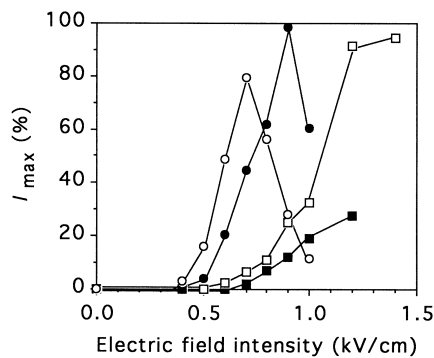


Fig. 2. Effect of long-pulse-electric field intensity on lucigenin-dependent chemiluminescence intensity. Cell suspensions ( $2\text{--}4 \times 10^8$  cells/ml) received one single electric pulse of 0.5 ms (■), 1 ms (□), 5 ms (●), and 10 ms (○) in lucigenin-containing buffer A.  $I_{\max}$  values were expressed as percentages of those obtained with one 5-ms pulse of 0.9 kV/cm. Average standard deviations on each point were about 10% and were not presented to prevent figure overloading.

value, any increase in the electric field strength led to an increase of the number of electroporabilised cells. A plateau value was reached for the longest pulse durations (5 and 10 ms). Fig. 2 shows the different chemiluminescence signal intensities observed when a CHO cell suspension was electropulsed using single ms pulse with variable electric strength. A chemiluminescence response was detected only when the cell suspension was electropulsed with field intensities higher than an apparent threshold value ( $E_{\text{ch}}(T)$ ).  $E_{\text{ch}}(T)$  depended on the pulse duration. Above this threshold value, any increase in the electric field strength led to an increase of chemiluminescence response. A plateau value was only reached when a 1-ms pulse was used. For longer pulse durations, the chemiluminescence response decreased when electric field intensity was higher than 0.6 and 0.9 kV/cm for one pulse of 10 and 5 ms, respectively (Fig. 2).

Influence of pulse duration on the  $E_{\text{ch}}(T)$  and  $E_{\text{p}}(T)$  values was analysed. Increasing the pulse duration resulted in a decrease in  $E_{\text{ch}}(T)$  and  $E_{\text{p}}(T)$  (Figs. 1 and 2). A linear relationship was found between the reciprocal of pulse duration and the apparent threshold values (Fig. 3). Extrapolation for infinite pulse duration allowed determination of the same critical threshold value equal to 0.44 kV/cm for the two processes.

### 3.2. Dependence of oxygen species generation on the short-term cell death resulting from electropulsation

Recovery of electroporabilised cell membrane integrity was observed 30 min after electropulsation. When using strong electric fields, a high membrane permeability to Direct-blue can still be present in the 15–20 min time range after pulsation. This irreversible membrane permeabilisation depicts the short-term cell death associated with strong electroporabilisation [22]. The occurrence of short-term cell death was simultaneous with the decrease in chemiluminescence response associated with strong electric field conditions, i.e. for a field strength of 0.6 kV/cm when one 10-ms pulse was applied (see Fig. 2). Above this field strength value, the higher the short-term cell death, the lower the chemiluminescence signal intensity (Fig. 4).

### 3.3. Dependence of long-term cell death resulting from electropulsation on the oxygen species generation

The long-term cell death was defined as the inability of pulsed cells to grow after electropulsation [22]. Long-term cell death was present as soon as cell electroporabilisation was triggered, i.e. when the electric field strength was higher than the apparent

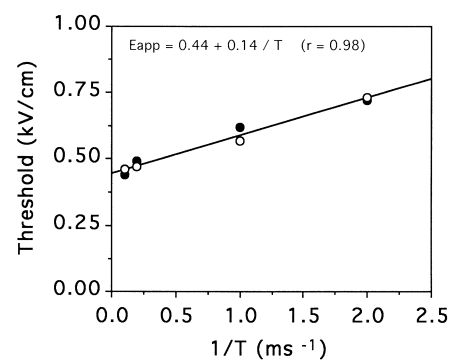


Fig. 3. Effect of pulse duration on apparent threshold values. CHO cell suspensions were pulsed by one single pulse with variable duration  $T$ . Apparent threshold values determined for different values of  $T$  were reported in relation to  $1/T$  in the case of electroporabilisation to Direct-blue (○) and chemiluminescence detection (●). Correlation coefficient of the straight line was 0.98. Extrapolation to infinite duration gave the same critical threshold value for electroporabilisation and CL (0.44 kV/cm).

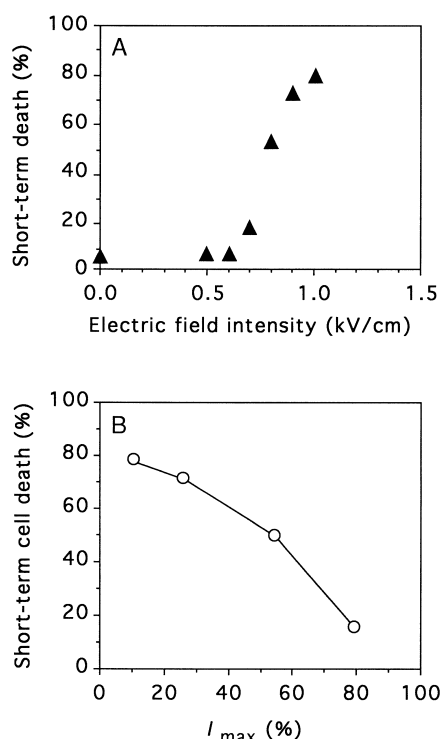


Fig. 4. Correlation between electro-induced short-term cell death and chemiluminescence signal intensity. Cell suspensions ( $10^7$  cells/ml) received one single electric pulse of 10 ms in buffer A with different field intensities. Short-term cell death was measured 20 min after electropulsation using Direct-blue exclusion assay. (A) Short-term cell death in relation to the applied electric field intensity. (B) Short-term cell death in relation to the lucigenin-dependent chemiluminescence intensity.  $I_{\max}$  values were from Fig. 2.

threshold  $E_p(T)$ . Above this threshold, the higher the field intensity, the higher the long-term cell death (Fig. 5).

Using one 10- or 5-ms pulse, data from CL intensity ( $I_{\max}$ ) and long-term cell death associated with different electric field intensities were correlated linearly (Fig. 6).

Fig. 7 shows the correlation between  $I_{\max}$  and long-term cell death obtained using three different electric field intensities (0.5, 0.6, and 0.7 kV/cm) for which low short-term cell death was present. For each electric field, three different electric conditions were used: one single pulse of 5 ms, one of 10 ms, and ten 100- $\mu$ s pulses applied with a frequency of 1 Hz. For the three electric field intensities, a linear relationship was found between  $I_{\max}$  and long-term cell death. The slope of the linear correlations was

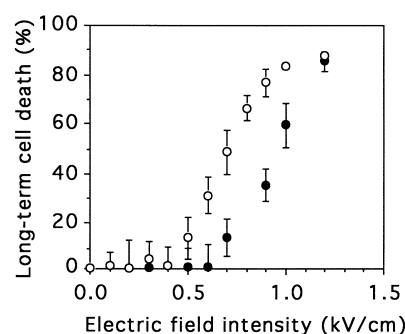


Fig. 5. Dependence of long-term cell death on the electric field intensity. Cell suspensions ( $2 \times 10^6$  cells/ml) received one single pulse of 5 ms (●) and 10 ms (○) in buffer A. Viability was measured by quantifying the ability of cells to grow as monolayers, over 24 h after electropulsation, by crystal violet assay. Long-term cell death was expressed as percentages of control.

the same whatever the electric field strength (correlation coefficients higher than 0.98).

We investigated the effect of an accumulation of  $\mu$ s pulses on long-term cell death and its correlation with the oxidative jump in regard to what was observed using ms pulses. Cells were electropulsed using an electric field intensity of 0.9 kV/cm, and keeping the total cumulated pulse duration equal to 10 ms ( $200 \times 50 \mu$ s,  $20 \times 500 \mu$ s,  $2 \times 5$  ms, and  $1 \times 10$  ms). For multiple pulses, the frequency was 1 Hz. Low short-term cell death was present using these electric conditions (smaller than 12%). Fig. 8 shows the correlation between oxidative jump amplitude ( $I_{\max}$ ) and

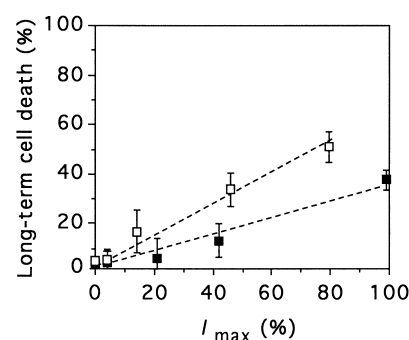


Fig. 6. Long-term cell death after electroporation in relation to the maximum chemiluminescence signal. Cell suspensions received one single pulse of 5 ms (■) and 10 ms (□) in buffer A, with different electric field intensities. Long-term cell death was expressed as in Fig. 5. 100% of  $I_{\max}$  was for cell electropulsation with one 5-ms pulse of 0.9 kV/cm intensity. The correlation coefficient of the two straight lines was higher than 0.97.

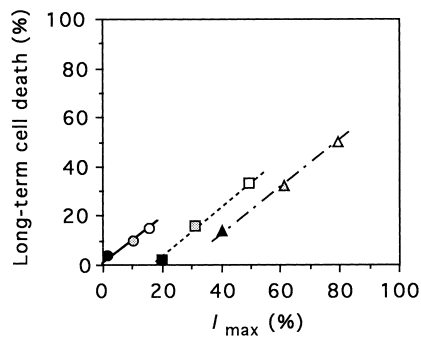


Fig. 7. Relationship between long-term cell death and chemiluminescence signal intensity. Cell suspensions received 10 100- $\mu$ s pulses (1 Hz frequency) (shaded symbols), one 5-ms pulse (open symbols), and one 10-ms pulse (closed symbols) in buffer A. Data were reported for three electric field strengths: 0.5 kV/cm (circles), 0.6 kV/cm (squares), and 0.7 kV/cm (triangles). Data for 10 100- $\mu$ s pulse conditions were from [36]. 100% of  $I_{\max}$  was for cell electropulsation with one 5-ms pulse of 0.9 kV/cm intensity.

long-term cell death obtained under these conditions. A break was observed beyond a 20-s treatment.  $I_{\max}$  remained constant while the long-term cell death was higher.

### 3.4. Analysis of the photo-oxidation kinetics of plasma membrane inserted (Pam)Afluorescein

The photo-oxidation kinetics of the fluorescent

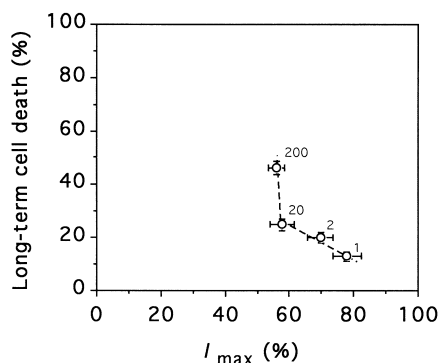


Fig. 8. Relationship between long-term cell death and chemiluminescence signal intensity when an accumulation of pulses with 10 ms-cumulated pulse duration was used. Cell suspensions received pulses of 0.9 kV/cm (1 Hz frequency) in buffer A with different numbers (1, 2, 20, and 200) and durations (10, 5, 0.5, and 0.05 ms), but with the same cumulated duration (10 ms). Each symbol was annotated with its corresponding number of pulses. For this work, experimental parameters were accordingly adjusted to a change in cell sensitivity to the electric field (see Section 2).

probe was analysed on the cell population, by measuring its fluorescence decay under continuous excitation. In our experimental conditions and when no electric field was applied, the decay during the first minute was representative of a first-order photo-oxidation reaction [22]. From the analysis of the (Pam)Afluorescein photo-oxidation kinetics (data not shown), we obtained an apparent photo-oxidation rate of  $0.62 \pm 0.06 \text{ min}^{-1}$ . The fluorescence decay was faster when cells were electroporated, showing an increase in the apparent (Pam)Afluorescein photo-oxidation rate. After labelled cell electroporation, the photo-oxidation reaction was of a first order during the first 20 s of illumination (data not shown). The apparent (Pam)Afluorescein photo-oxidation rate was estimated as  $1.15 \pm 0.1 \text{ min}^{-1}$  for one 5-ms pulse of 0.9 kV/cm. This apparent rate depicted the photo-oxidation processes of three cell sub-populations, i.e. the non-electroporated cells, the living electroporated cells, and the irreversibly permeabilised (dead) cells (see Appendix B). The rate constant of (Pam)Afluorescein inserted in the electroporated membrane parts was  $2.57 \text{ min}^{-1}$ , i.e. 4 times higher than the one inserted in the native membrane ( $0.62 \text{ min}^{-1}$ ).

## 4. Discussion

A generation of ROS was triggered when suspended CHO cells were electroporated using electric field with long-lasting pulse duration. This oxidative jump was not due to electrode electrochemistry or to Joule heating [18]. The electro-induced oxidative jump was only observed when the electric field strength applied through the cell suspension was higher than an apparent threshold value which depended on the pulse duration (Fig. 2) as in electroporation (Fig. 1). The critical threshold value was the same for electro-induced ROS generation and electroporation (0.44 V/cm, Fig. 3), i.e. the two phenomena were simultaneously triggered. This was previously reported using  $\mu$ s pulses with CHO cells [18] and with human erythroleukaemia K562 cells [34]. The oxidative jump appears to be a consequence of the permeabilised state of the plasma membrane. This assumption was supported by the membrane localisation of the reactive-oxygen species

as depicted by the increase of the photo-oxidation rate of (Pam)Afluorescein when inserted in the electroporabilised cell membrane (present results and [22]) and by the increase of the lipid peroxidation after electroporabilisation [23].

When long pulses were used (5 and 10 ms), a decrease of the CL was observed for higher electric field strengths (Fig. 3). This observation agreed with previous work on peritoneal macrophages [14]. The authors showed that the electro-induced chemiluminescence of macrophages diminished to zero when the cells were exposed to high electric field pulses. Light-scattering analysis of the macrophage suspension at a high electric field intensity indicated irreversible alteration of the barrier function of the phagocyte membrane. This indicated irreversible membrane rupture associated with annihilation of the trans-membrane potential difference [35]. Such irreversible alteration of the membrane barrier function was observed with CHO cell under stringent pulsing conditions and was defined as short-term cell death [36]. The higher the short-term cell death level, the higher the decrease in the CL signal (Fig. 4). This observation supported the hypothesis that the electro-induced membrane state governed the yield of the ROS generation. Electric field-induced ROS generation occurred only when the electroporabilised state of the cell membrane was reversible, i.e. when the long-term cell integrity was preserved. On the other hand, membrane physical changes associated with short-term cell death inhibited ROS generation [14]. Our results gave support to the assumption that cellular response to electric treatment might rely on enzymatic activities requiring cell integrity [34]. It was shown that the generation of ROS was preceded by membrane hyperpolarisation in human granulocytes [37], and was controlled by the trans-membrane potential in human macrophages [38]. NADPH-oxidase system has been previously identified in human [39,40] and hamster [41] fibroblasts. Our results could be explained by the effect of the trans-membrane potential difference changes associated with the electroporabilised state on membrane NADPH-oxidase system activity. This activity was not present in irreversibly damaged cells where this electric parameter was brought to zero. Previous works showed that electric field-induced changes in trans-membrane potential differences affect the properties of plasma membrane

channels and pumps via electro-conformational changes [42–45].

Localised activation of membrane NADPH oxidase in fibroblasts could be triggered on the cell surface by mechanical intrusion [46]. ROS generated by electroporabilised CHO cells were localised only in the permeabilised part of the plasma membrane, [22] as proved by the associated local strong activating effect on (Pam)Afluorescein photo-oxidation reaction. The rate constant of the reaction occurring in the electroporabilised membrane parts ( $k_2$ ) was 1.8 and 4 times higher than the control one ( $k_1$ ), when the cells were previously electroporabilised using 1- and 5-ms cumulated duration pulse, respectively (see Appendix B).  $k_2$  increased when the cumulated pulse duration was increased. When the pulse duration was smaller than 1 ms, the oxidative jump intensity depended linearly on this parameter [18]. A saturation in the oxidative response was present when the pulse duration was increased over 1 ms. For CHO cells pulsed using one pulse of 0.9 kV/cm,  $I_{\max}$  values were 30 and 65% for pulse duration of 1 and 5 ms, respectively [18]. Such saturation was also observed with  $k_2$  values. The increase of  $k_2$  was directly correlated to the increase of the ROS generation yield when the pulse duration was increased ( $1.8/4 = 30/65$ ). Our observations pointed out that the long-term behaviour of the pulsed cell was different when short- and long-lasting pulses were used. This supported that mechanisms of membrane permeabilisation using short pulse and long pulse were fundamentally different [12,25] and that the role of the pulse duration was crucial in the electro-mediated cell processes (e.g. electro-mediated gene transfer).

The oxidative jump was not a simple passive feedback effect of membrane electroporabilisation. It strongly controlled cell survival (Fig. 6) [18]. The oxidative jump was explained by stress associated with the local changes in plasma membrane organisation. These changes allowed electroporabilisation, dependence of which on electric pulse parameters was at that time clearly described [7,9,11,47]. The part of the cell membrane globally affected by the electric treatment depended on the electric field strength while the extent of permeabilisation in this area depended on the duration and on the number of pulses. For a given cell surface affected by the treat-

ment (i.e. a given electric field strength), the long-term cell death linearly depended on the oxidative jump intensity (Fig. 7) as expected if the ROS generation process associated with electro-induced membrane alterations were involved in cell survival. This linear dependency was the same whatever the part of the cell surface affected by the electric treatment (Fig. 7). When reversibly permeabilising long-lasting pulses were used (as for electrically mediated gene transfer), the long-term cell survival was controlled by the amplitude of the oxidative jump.

However, results obtained with repetitive short pulses (Fig. 8) illustrated the complexity of the cellular responses associated with living cell electroporation. An accumulation of a large number of short pulses ( $\mu\text{s}$ ) was extremely lethal for cells, while no correlation with any increase in the oxidative jump amplitude was found (Fig. 8). This observation implied that other death-inducing factors than the oxidative jump were involved. The rotation rate of suspended CHO cells in buffer A has been evaluated from Einstein's relation to be about  $5 \text{ ms}^{-1}$  (i.e. 200 s for a complete rotation of the cell). When CHO cells were pulsed using repetitive short pulses with a frequency of 1 Hz, cells had significant time to rotate during the total time of the treatment. Consequently, cells were affected by the electric field in different parts of the cell membrane. In these conditions, the electrical treatment triggered low alterations in the membrane, but over a large fraction of the cell surface. Other cell death-inducing factors might be involved, such as mechanical stress due to local cell membrane electro-deformation [25,48] or irreversible damage in cellular functions [49]. Electroporation of the CHO cell membrane induced leakage of intracellular metabolite, such as ATP [11]. The membrane recovery process after electroporation of mammalian cells depended on the cellular energy state (characterised by the ATP level in the cell [50,51]). When using electrical treatment with long cumulative duration, the electro-induced leakage brought the intracellular content in nucleotides down significantly. Such nucleotide depletion could be a cell death-inducing factor independently of the oxidative jump.

Under electrical conditions needed for gene transfer (long pulse with high permeabilisation), the long-term cell death resulting from plasma membrane

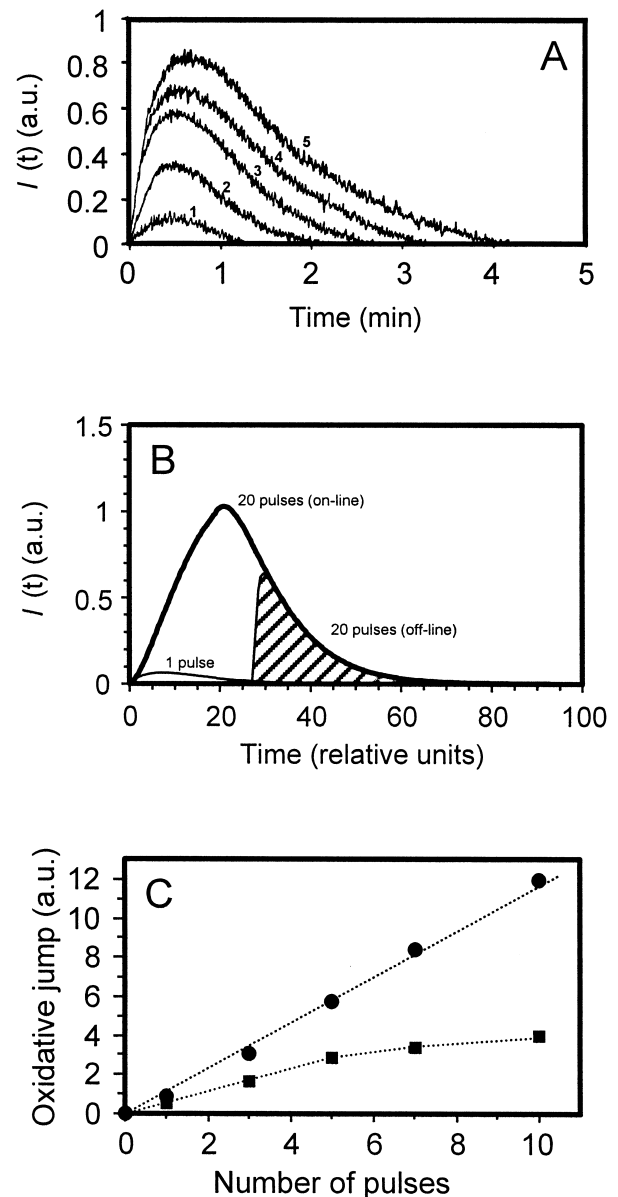


Fig. 9. Effect of a train of short pulses on the shape of the on-line CL signal. (A) On-line CL signals obtained when cells received one (1), three (2), five (3), seven (4), and ten (5) 100- $\mu\text{s}$  pulses in buffer A (1 Hz frequency) with an electric field strength of 1.4 kV/cm. (B) Graphic resolutions of Eq. 1 and Eq. 2 (one pulse and 20 pulses, respectively). Values of  $h_1$  and  $h_2$  are  $0.005 \text{ s}^{-1}$  and  $0.025 \text{ s}^{-1}$ , respectively. The shaded signal represents the underestimated signal measured off-line when 20 pulses were applied, i.e. about 15 s after the end of the last electric pulse (see Section 2). Simulations were obtained using Microsoft Excel 7.0a software (Microsoft). (C) Effect of the number of pulses on the parameters of the on-line CL signal. ■,  $I_{\text{max}}$  value; and ●, total area of the signal.

electropermeabilisation was correlated with the oxidative jump. But our results revealed the complexity of the living cell electropermeabilisation process. The oxidative jump amplitude associated with ms electropermeabilising pulse is related to the size of the membrane region electrically affected (defined by the electric field intensity). However, the electro-induced generation of ROS is affected by the short-term cell death present when using such long pulses. For electric fields which preserved short-term cell survival, the oxidative jump amplitude increases with the extent of alterations allowing permeabilisation. These perturbations are governed by the duration of the pulse. Our results show that when using ms pulses, the oxidative jump is induced only when cell electropermeabilisation is reversible. However, application of  $\mu$ s pulse trains with ms-cumulated duration is extremely lethal for cells while no correlation with the electro-induced oxidative jump is found. Other processes must be involved in electro-induced cell death mechanisms.

This transient state of the electropermeabilised cell could not be simply described as reversible free exchange mediated by lipidic cylindrical pores [35]. Metabolic cell responses, such as oxidative stress, were present and must be clearly understood in order to define the electric field-mediated gene transfer conditions allowing better cell survival. Use of reactive-oxygen species scavengers might increase the electro-mediated gene delivery efficiency significantly [52].

## Acknowledgements

We thank Mrs C. Millot for cell culture and Mr J. Robb who checked the English syntax. This work was partly supported by a grant from Electricité De France (EDF) 'Service des Études Médicales' (J.T.).

## Appendix A. Detection of CL when repetitive short pulses were applied with a 1-Hz frequency

The CL signal recorded on-line depends on the number of pulses applied on the cell suspension (Fig. 9A). When a train of short pulses is applied

with a frequency of 1 Hz and a total cumulated duration of 10 ms, the total time of the electropulsation assay is long (e.g. 200 s for 200 50- $\mu$ s pulses and 20 s for 20 500- $\mu$ s pulses). Using off-line detection of the CL signal (see Section 2), a significant delay (from 15 to 215 s) separates the on-set of the electropulsation from CL detection (Fig. 9B). This gives an underestimation of CL emission.

The full CL signal experimentally obtained using one single pulse is fitted using two exponentials:

$$I_1(t) = (1 - e^{-h_1 t})e^{-h_2 t} \quad (1)$$

in which  $(1 - e^{-h_1 t})$  depicts the lag which is detected in the onset of the CL signal [18]. The light emission relaxation is fitted to a single exponential ( $e^{-h_2 t}$ ) which was previously associated with the membrane recovery [18].

When  $n$  short pulses are applied with a frequency of 1 Hz and assuming that each pulse triggers ROS generation independently, we obtain:

$$I_n(t) = \sum_{j=0}^{j=(n-1)} (1 - e^{-h_1 [t-jD]})e^{-h_2 [t-jD]} \quad (2)$$

in which  $D$  is the delay between each pulse (i.e. 1 s) and  $t$  is the time from the beginning of the pulsation. This is valid under the assumption that there are no short-term cell death, which is induced by the pulses. In fact, there is a number of pulse-dependent short-term cell death. This means that in Eq. 2 there are less viable cells for long values of  $j$ , i.e. less cells able to generate ROS when electropermeabilised. The short-term cell death depends on the pulsing conditions and increases with the number of pulses. Eq. 1 and Eq. 2 are plotted for  $n=1$  or  $n=20$ , i.e. when one or 20 pulses are applied, respectively (Fig. 9B). Rate constants are chosen as  $h_1 = 0.005 \text{ s}^{-1}$ ,  $h_2 = 0.025 \text{ s}^{-1}$ . They are associated with short pulse duration (several  $\mu$ s). When multiple pulses are applied, there is no direct addition of  $I_{\max}$  values associated with each single pulse (Fig. 9C). The signal which is measured off-line is only the final decay and does not represent the real ROS generation associated with electropermeabilisation (Fig. 9B). However, when CL is detected on-line, there is direct addition of the signals associated with each individual pulse (Fig. 9C). Therefore, when repetitive short pulses are used, we quantify the on-line CL signal by

its total area (Fig. 9C). This is associated with the total ROS generation.

## Appendix B. Determination of the rate constants of (Pam)Afluorescein in the native and electroporated part of the cell membrane

The (Pam)Afluorescein photo-oxidation can be depicted as a pseudo-first order reaction [22] with an apparent rate constant  $k_{ox}$ :

$$I_f(t) = I_f(0)e^{-k_{ox}t} \quad (3)$$

in which  $I_f(t)$  and  $I_f(0)$  are the fluorescence intensities of the recorded signal measured at time  $t$  and at the beginning of the photo-oxidation reaction, respectively. When the labelled CHO cell suspension was previously electroporated, the recorded fluorescence decay depicts the photo-oxidation processes of three cell sub-populations, i.e., the living electroporated cells, the irreversibly permeabilised cell (dead cell), and the living non-electroporated cells. We assume that short-term cell death was an exclusive consequence of the electric field-mediated membrane permeability. Then we can write:

$$I_f(t) = I_{fp}(t) + I_{fd}(t) + I_{fo}(t) \quad (4)$$

in which  $I_{fp}(t)$ ,  $I_{fd}(t)$ ,  $I_{fo}(t)$  are the fluorescence intensities at time  $t$  associated with the living electroporated cells, the irreversibly permeabilised cells (short-term dead cells), and the non-electroporated cells (i.e. as the control cells), respectively. Assuming that the (Pam)Afluorescein photo-oxidation is a first-order reaction whatever the cell sub-population we consider, but with specific rate constants, Eq. 3 converts to:

$$I_f(t) = I_f(0)[(p + v - 1)e^{-k_p t} + (1 - v)e^{-k_d t} + (1 - p)e^{-k_o t}] \quad (5)$$

in which  $p$  is the cell population fraction which is electroporated,  $v$  is short-term viable one, and  $k_p$ ,  $k_d$  and  $k_o$  are the photo-oxidation rate constants associated with the living electroporated cells, the irreversibly permeabilised ones, and the native control ones, respectively.

From [18] and because cell membrane electropor-

ation is a dissymmetrical event under our conditions [7], we have:

$$I_{fp}(t) = I_f(0)e^{-k_p t} = I_f(0)/2\{[E_s/E + E_F/E]e^{-k_1 t} + [(1 - E_s/E) + (1 - E_F/E)]e^{-k_2 t}\} \quad (6)$$

in which  $k_1$  and  $k_2$  are the photo-oxidation rate constants in the non-electroporated and the electroporated membrane areas, respectively;  $E_s$  and  $E_F$  are the critical electric field intensity thresholds upward from which cell electroporation is triggered on the side facing the anode and facing the cathode, respectively; and  $E$  is the electric field strength applied on the cell suspension.  $k_2$  reflects the enhancement of the photo-oxidation process due to the local ROS generation.

The oxidative jump is only associated with the localised reversible electroporation (see text), therefore  $k_d$ ,  $k_o$  and  $k_1$  are the same rate constant. Then, Eq. 5 and Eq. 6 give:

$$I_f(t)/I_f(0) = (p + v - 1)/2\{(E_s/E + E_F/E)e^{-k_1 t} + [(1 - E_s/E) + (1 - E_F/E)]e^{-k_2 t}\} + (1 - v)e^{-k_1 t} + (1 - p)e^{-k_1 t} \quad (7)$$

The oxidation rate constants can be determined from the slope at time  $t = 0$ , i.e.,  $[dI_f(t)/dt]_{t=0}$ . From Eq. 3 and Eq. 7, we obtain:

$$k_{ox} = 1/2\{(p + v - 1)(E_s/E + E_F/E) + (4 - 2v - 2p)k_1 + (p + v - 1)[(1 - E_s/E) + (1 - E_F/E)]k_2\} \quad (8)$$

When CHO cells were pulsed using one 5-ms pulse with  $E = 0.9$  kV/cm (this work),  $k_{ox}$  and  $k_1$  were estimated as 1.15 and 0.62 min<sup>-1</sup>, respectively. With these electrical conditions, we had  $p = 1$ ,  $v = 0.8$ ,  $E_s = 0.44$  kV/cm, and  $E_F = 0.75$  kV/cm. From Eq. 8, we calculate  $k_2 = 2.57$  min<sup>-1</sup>, i.e. 4 times higher than  $k_1$ , when one 5-ms pulse was applied. When CHO cells were pulsed using a 1-ms cumulated-duration pulse (10 100-μs pulses) with  $E = 0.9$  kV/cm [22],  $k_{ox}$  and  $k_1$  were estimated as 0.8 and 0.68 min<sup>-1</sup>, respectively. With these electrical conditions, we had  $p = 0.75$ ,  $v = 0.9$ ,  $E_s = 0.44$  kV/cm, and  $E_F = 0.75$  kV/cm. From Eq. 8, we calculate  $k_2 = 1.22$  min<sup>-1</sup>, i.e.

1.8 times higher than  $k_1$ , when a 1-ms cumulated-duration pulse was applied.

## References

- [1] I. Hapala, *Crit. Rev. Biotechnol.* 17 (1997) 105–155.
- [2] R.O. Potts, Y.A. Chizmadzhev, *Nat. Biotechnol.* 16 (1998) 135.
- [3] L.M. Mir, P. Devauchelle, F. Quintin-Colonna, F. Delisle, S. Doliger, D. Fradelizi, J. Belehradek Jr., S. Orlowski, *Br. J. Cancer* 76 (1997) 617–1622.
- [4] M.P. Rols, C. Delteil, M. Golzio, P. Dumont, S. Cros, J. Teissié, *Nat. Biotechnol.* 16 (1998) 168–171.
- [5] M.R. Prausnitz, *Crit. Rev. Ther. Drug Carrier Syst.* 14 (1997) 455–483.
- [6] P. Marszalek, D.S. Liu, T.Y. Tsong, *Biophys. J.* 58 (1990) 1053–1058.
- [7] B. Gabriel, J. Teissié, *Biophys. J.* 73 (1997) 2630–2637.
- [8] E. Neumann, B. Rosenheck, *J. Membr. Biol.* 10 (1972) 279–290.
- [9] K. Schwister, B. Deuticke, *Biochim. Biophys. Acta* 816 (1985) 332–348.
- [10] B. Gabriel, J. Teissié, *Eur. Biophys. J.* 27 (1998) 291–298.
- [11] M.P. Rols, J. Teissié, *Biophys. J.* 58 (1990) 1089–1098.
- [12] M.P. Rols, J. Teissié, *Biophys. J.* 75 (1998) 1415–1423.
- [13] G.K. Smith, S.F. Cleary, *Biochim. Biophys. Acta* 763 (1983) 325–331.
- [14] E.M. Annaberdyeva, I.G. Polnikov, T.V. Puchkova, V.S. Sharov, A.V. Putvinski, *Biull. Eksp. Biol. Med.* 103 (1987) 452–453.
- [15] F. Bobanovic, S. Simcic, V. Kotnik, L. Vodovnik, *FEBS Lett.* 331 (1992) 95–98.
- [16] V.S. Malinin, V.S. Sharov, A.V. Putvinsky, A.N. Osipov, Y.A. Vladimirov, *Bioelectrochem. Bioenerg.* 22 (1989) 37–44.
- [17] V.S. Malinin, K.D. Kazarinov, A.V. Putvinsky, *Biofizika* 41 (1996) 876–886.
- [18] B. Gabriel, J. Teissié, *Eur. J. Biochem.* 223 (1994) 25–33.
- [19] M. Maccarrone, N. Rosato, A. Finazzi Agrò, *Biochem. Biophys. Res. Commun.* 206 (1995) 238–245.
- [20] N. Sabri, B. Pelissier, J. Teissié, *Eur. J. Biochem.* 238 (1996) 737–743.
- [21] B. Galutzov, V. Ganeva, *Bioelectrochem. Bioenerg.* 44 (1997) 77–82.
- [22] B. Gabriel, J. Teissié, *Eur. J. Biochem.* 228 (1995) 710–718.
- [23] M. Maccarrone, M.R. Bladergroen, N. Rosato, *Biochem. Biophys. Res. Commun.* 209 (1995) 417–425.
- [24] E. Neumann, M. Schäfer-Ridder, Y. Yang, P. Hofschneider, *EMBO J.* 1 (1982) 841–845.
- [25] J. Akinlaja, F. Sachs, *Biophys. J.* 75 (1998) 247–254.
- [26] R.T. Kubiniec, H. Liang, S.W. Hui, *Biotechniques* 8 (1990) 16–21.
- [27] T. Xie, T.Y. Tsong, *Biophys. J.* 63 (1992) 28–34.
- [28] C. Baum, P. Forster, S. Hegewisch-Becker, K. Harbers, *Biotechniques* 17 (1994) 1058–1062.
- [29] N. Eynard, M.P. Rols, V. Ganeva, B. Galutzov, N. Sabri, J. Teissié, *Bioelectrochem. Bioenerg.* 44 (1997) 103–110.
- [30] W.S. Meaking, J. Edgerton, C.W. Wharton, R.A. Meldrum, *Biochim. Biophys. Acta* 1264 (1995) 357–362.
- [31] C.S. Djuzenova, V.L. Sukhorukov, G. Klock, W.M. Arnold, U. Zimmermann, *Cytometry* 15 (1995) 35–45.
- [32] M.A. Tsai, R.E. Waugh, P.C. Keng, *Biophys. J.* 70 (1996) 2023–2029.
- [33] W. Kueng, E. Silber, U. Eppenberger, *Anal. Biochem.* 182 (1989) 16–19.
- [34] M. Maccarrone, C. Fantini, A. Finazzi Agrò, N. Rosato, *Biochim. Biophys. Acta* 1414 (1998) 43–50.
- [35] J.C. Weaver, A. Chizmadzhev, *Bioelectrochem. Bioenerg.* 42 (1996) 135–160.
- [36] B. Gabriel, J. Teissié, *Biochim. Biophys. Acta* 1266 (1995) 171–178.
- [37] H.M. Korchak, G. Weissmann, *Proc. Natl. Acad. Sci. USA* 75 (1978) 3818–3822.
- [38] H. Schmid-Antomarchi, A. Schmid-Alliana, G. Romey, M.A. Ventura, V. Breittmayer, M.A. Millet, H. Husson, B. Moghrabi, M. Lazdunski, B. Rossi, *J. Immunol.* 159 (1997) 6209–6215.
- [39] B. Meier, A.R. Cross, J.T. Hancock, F.J. Kaup, O.T. Jones, *Biochem. J.* 275 (1991) 241–245.
- [40] S. Arbault, P. Pantano, N. Sojic, C. Amatore, M. Best-Belhomme, A. Sarasin, M. Vuillaume, *Carcinogenesis* 18 (1997) 569–574.
- [41] J.E.M. Souren, H.V. Aken, R.V. Wijk, *Biochem. Biophys. Res. Commun.* 227 (1996) 816–821.
- [42] J. Teissié, T.Y. Tsong, *J. Membr. Biol.* 55 (1980) 133–140.
- [43] T.Y. Tsong, *Bioelectrochem. Bioenerg.* 24 (1990) 271–295.
- [44] W. Chen, R.C. Lee, *Biophys. J.* 67 (1994) 603–612.
- [45] W. Chen, Y. Han, Y. Chen, D. Astumian, *Biophys. J.* 75 (1998) 196–206.
- [46] S. Arbault, P. Pantano, J.A. Jankowski, M. Vuillaume, C. Amatore, *Anal. Chem.* 67 (1995) 3382–3390.
- [47] J. Teissié, C. Ramos, *Biophys. J.* 74 (1998) 1889–1898.
- [48] G.V. Gass, L.V. Chernomordik, L.B. Margolis, *Biochim. Biophys. Acta* 1093 (1991) 162–167.
- [49] M.C. Vernhes, P.A. Cabanes, J. Teissié, *Bioelectrochem. Bioenerg.* 48 (1999) 17–25.
- [50] H. Kosowski, R. Matthias, L. Schild, W. Halangk, *Bioelectrochem. Bioenerg.* 38 (1995) 377–381.
- [51] M.P. Rols, C. Delteil, M. Golzio, J. Teissié, *Eur. J. Biochem.* 254 (1998) 382–388.
- [52] N. Sabri, B. Pelissier, J. Teissié, *Anal. Biochem.* 264 (1998) 284–286.